European Journal of Immunology Clinical·Basic·Translational

Immunodeficiencies and autoimmunity

Clinical

Research Article

Differential Runx3, Eomes, and T-bet expression subdivides MS-associated CD4$^+$ T cells with brain-homing capacity

Cindy Hoeks[1,2], *Fabiënne van Puijfelik*[3], *Steven C. Koetzier*[3], *Jasper Rip*[3], *Cato E.A. Corsten*[4], *Annet F. Wierenga-Wolf*[3], *Marie-José Melief*[3], *Piet Stinissen*[1,2], *Joost Smolders*[3,4,5], *Niels Hellings*[1,2], *Bieke Broux*[1,2] *and Marvin M. van Luijn*[3]

[1] Department of Immunology and Infection, Biomedical Research Institute, Hasselt University, Hasselt, Belgium
[2] University MS Center (UMSC), Hasselt, Belgium
[3] Department of Immunology, MS Center ErasMS, Erasmus MC, University Medical Center Rotterdam, Rotterdam, the Netherlands
[4] Department of Neurology, MS Center ErasMS, Erasmus MC, University Medical Center Rotterdam, Rotterdam, the Netherlands
[5] Neuroimmunology Research Group, Netherlands Institute for Neuroscience, Amsterdam, the Netherlands

Multiple sclerosis (MS) is a common and devastating chronic inflammatory disease of the CNS. CD4$^+$ T cells are assumed to be the first to cross the blood–central nervous system (CNS) barrier and trigger local inflammation. Here, we explored how pathogenicity-associated effector programs define CD4$^+$ T cell subsets with brain-homing ability in MS. Runx3- and Eomes-, but not T-bet-expressing CD4$^+$ memory cells were diminished in the blood of MS patients. This decline reversed following natalizumab treatment and was supported by a Runx3$^+$Eomes$^+$T-bet$^-$ enrichment in cerebrospinal fluid samples of treatment-naïve MS patients. This transcription factor profile was associated with high granzyme K (GZMK) and CCR5 levels and was most prominent in Th17.1 cells (CCR6$^+$CXCR3$^+$CCR4$^{-/dim}$). Previously published CD28$^-$ CD4 T cells were characterized by a Runx3$^+$Eomes$^-$T-bet$^+$ phenotype that coincided with intermediate CCR5 and a higher granzyme B (GZMB) and perforin expression, indicating the presence of two separate subsets. Under steady-state conditions, granzyme K^{high} Th17.1 cells spontaneously passed the blood–brain barrier *in vitro*. This was only found for other subsets including CD28$^-$ cells when using inflamed barriers. Altogether, CD4$^+$ T cells contain small fractions with separate pathogenic features, of which Th17.1 seems to breach the blood–brain barrier as a possible early event in MS.

Keywords: Pathogenic CD4$^+$ T cells · Th17.1 · CD4$^+$CD28$^-$ · Runx3 · Eomes · T-bet · Multiple sclerosis

Additional supporting information may be found online in the Supporting Information section at the end of the article.

Correspondence: Dr. Marvin M. van Luijn
e-mail: m.vanluijn@erasmusmc.nl

[*] Steven C. Koetzier is currently working at the Department of Transplantation Immunology, Maastricht University Medical Center+, Maastricht, Netherlands
[**] Cindy Hoeks, Fabiënne van Puijfelik, and Steven C. Koetzier contributed equally as first authors.
[‡] Bieke Broux and Marvin M. van Luijn contributed equally as senior authors.

Introduction

Multiple sclerosis (MS) is the most prevalent nontraumatic cause of neurological disability among young adults. Although the etiology of MS is still unclear, studies have highlighted that certain pathogenic T cells are induced in peripheral lymphoid organs to infiltrate the CNS and trigger local inflammation and demyelination. $CD4^+$ T cells are enriched in the cerebrospinal fluid (CSF) and are considered one of the first immune cells that disrupt and cross the blood–brain barrier (BBB) in MS [1, 2]. More in-depth insights into the effector program of brain-homing $CD4^+$ T cells in people with MS are needed to better understand which subsets are triggered and how these affect the BBB as an initial event in the disease course [3, 4]. The obtained knowledge can help to fine-tune and personalize the use of currently available T-cell-directed treatments and to develop more refined therapeutic strategies that only target the disease-relevant T-cell subsets [5–7].

As described by a vast body of literature, $CD4^+$ T cells can be classified into various subsets based on the expression of lineage-specifying transcription factors (TF), distinct chemokine receptors, and signature pro-inflammatory mediators, all of which allow these T-cell subsets to exert different effectors functions in inflamed tissues such as the CNS in MS [8–10]. The complexity of this classification is ever-increasing as several new $CD4^+$ T-cell phenotypes are being identified, with characteristics that likely overlap between subsets [11]. We have previously reported on two specialized $CD4^+$ T-cell subsets that are associated with the disease process of MS, namely $CD4^+CD28^-$ [12] and Th17.1 ($CCR6^+CXCR3^+CCR4^{-/dim}$) cells [13].

Human $CD4^+CD28^-$ T cells, also known as $CD28^{null}$ T cells, are clonally restricted and terminally differentiated helper T cells. This subset is not only characterized by a loss of co-stimulatory receptor CD28 but also by a gain of natural killer (NK) receptors and cytotoxic molecules such as perforin and granzyme B [14–17] (see [18] for a recent review) and by resistance to Treg-mediated suppression [12, 19]. Cytotoxic properties of $CD4^+CD28^-$ cells have been described in the context of cardiovascular diseases, rheumatoid arthritis [20], and neuroinflammation [21, 22]. In MS patients, expansion of circulating $CD4^+CD28^-$ T cells is associated with accelerated disease progression [23]. Furthermore, this subset has the capacity to infiltrate inflammatory sites and accumulate in MS brain lesions [21, 24–26].

Although Th17.1 cells are less familiar, we and others have provided several lines of evidence that this T-cell subset contributes to chronic inflammatory diseases such as MS. For instance, as compared with other $CD4^+$ memory T cells, Th17.1 cells selectively express antiapoptotic and cytotoxicity-related genes, and are highly insensitive to glucocorticoids [13, 27, 28]. Furthermore, Th17.1-like cells are cytotoxic toward oligodendrocytes [29] and drive the pathology of experimental autoimmune encephalomyelitis, the most commonly used animal model for MS [30]. In people with MS, Th17.1 cells were relatively less present in blood during active disease, particularly accumulated in the blood after anti-VLA-4 treatment (natalizumab [NTZ]; preventing the entry into the CNS) and predominated the CSF in contrast to controls [13, 28, 31].

To understand whether Th17.1 and $CD4^+CD28^-$ T cells differentially contribute to MS, it is critical to assess the extent to which their effector program overlaps and how this is associated with a brain-homing phenotype. For $CD8^+$ cytotoxic T cells (CTLs), the effector program is defined by a close interplay between runt-related transcription factor 3 (Runx3) and T-box transcription factors Eomesodermin (Eomes) and T-bet. [32–34]. In this study, we integrated co-expression profiles of these transcription factors with those of effector molecules (GZMB, GZMK, perforin) and chemokine receptors (CCR6, CXCR3, CCR5) to define the brain-homing phenotype of $CD4^+$ memory T cells in MS. For this, we used blood samples from healthy individuals and MS patients with and without NTZ treatment. Results of these immunophenotypic analyses were confirmed *ex vivo* using paired MS blood and CSF samples and *in vitro* using both inflamed and noninflamed brain endothelial layers, with a specific focus on Th17.1 and $CD4^+CD28^-$ T cells. Taken together, our data show that the expression of Runx3, Eomes, and T-bet characterizes $CD4^+$ memory T cells with distinct brain-homing potential, which is different between Th17.1 and $CD4^+CD28^-$ T cells and reveals potential new avenues for specifically targeting these subsets during the MS course.

Materials and methods

Study subjects

Peripheral blood samples were collected from healthy donors in collaboration with the University Biobank Limburg (UBiLim). We obtained paired blood and CSF samples of MS patients who did not receive disease-modifying therapy and were included at MS center ErasMS (Erasmus MC). In addition, blood samples were collected from MS patients with a relapsing-remitting disease course who did and did not receive 18 months of NTZ treatment. None of the NTZ-treated patients experienced a clinical relapse. All patients were diagnosed according to the McDonald 2017 criteria [35] and samples were collected at the time of diagnosis. This study was approved by the local ethical committees (Erasmus MC, UBiLim Hasselt) and informed consent was obtained from all donors. Clinical information of donors can be found in Table 1.

Cell isolation

PBMC were isolated from whole blood using either density gradient centrifugation (Lympholyte; Cedarlane) for samples collected by UBiLim, or using CPT tubes (BD Biosciences) with sodium heparin for samples collected by Erasmus MC. Obtained PBMC were either used fresh or were frozen in fetal bovine serum (FBS; Gibco, Thermo Fisher Scientific) with 10% DMSO (Sigma-Aldrich) at UBiLim, or in RPMI 1640 with L-Glutamine

Table 1. Clinical information of donors used for this study.

Cohort (sample)	HC (PB)	MS (PB)	NTZ-MS (PB)	MS (PB + CSF)
Number	18	17	8	9
Sex (M/F)	10/8	8/9	4/4	5/4
Age (range) ± SEM	38.6 (26–57) ± 1.865	39.6 (23–48) ± 1.649	30.0 (19–39) ± 18.394	46 (20–62) ± 5.406
Treatment	N/A	No DMT, MP <1-month prior sampling 3/18 No treatment 15/18	18 months with natalizumab 8/8	No DMT, MP <1-month prior sampling 1/9 No treatment 8/9

Note: Donors mentioned in column denoted "PB + CSF" are MS patients from which paired peripheral blood (PB) and cerebrospinal fluid (CSF) samples were analyzed.
Abbreviations: HC, healthy controls; MS, multiple sclerosis; NTZ, natalizumab; MP, methylprednisolone; N/A, not applicable.

(Lonza) with 20% FBS and 10% DMSO at Erasmus MC. PBMC were stored in liquid nitrogen until further use. Paired blood and CSF samples from MS patients were collected on the same day and measured immediately upon collection and processing. PBMC isolated to be used in migration assays were sorted on the same day the blood was collected and were immediately used for migration assays. All remaining experiments were performed using frozen material.

Flow cytometry

For *ex vivo* sorting and phenotyping, the following antibodies were used: CD4 BV605, CD8 AF700, CD28 BV711, CD45RA APC Fire750 and BV605, CD45RO BV650, CD69 BV421, CCR4 PE Cy7, CCR5 AF700, CCR6 PE, CCR6 BV650, CXCR3 APC, CXCR3 BV785, granzyme B AF647, granzyme K FITC, perforin BV421, T-bet PerCP-Cy5.5, Runx3 PE (all BioLegend), granzyme B PE-CF594, Fixable viability dye 700 (both BD Biosciences), CD4 APC eFluor780, Perforin PerCP eFluor710, Eomes PE eFluor610, Fixable viability dye eFluor506 (all Thermo Fisher Scientific). Intracellular staining was performed using the BD Pharmingen Transcription Factor buffer set (BD Biosciences). Our gating strategy used to identify Th subsets (based on [13, 27, 36, 37] is shown in Fig. S1). The purity of all cell sorts was confirmed to be >95%. Cells were sorted using a FACSAria Fusion and phenotyped using a BD LSRFortessa. Flow cytometry data were manually analyzed using FACSDiva 8.0.2 or FlowJo 10.8.1 (all from BD Biosciences). Samples with <100 events within the analyzed gate were excluded from the analysis to ensure high-quality data. FlowSOM and opt-SNE analysis of the median fluorescent intensity was performed using OMIQ software from Dotmatics (www.omiq.ai, www.dotmatics.com).

Boyden chamber migration assay

Positive selection of $CD3^+$ T cells using magnetic beads was performed prior to sorting according to the manufacturer's protocol (MojoSort Human CD3 selection kit, BioLegend). For Boyden chamber migration assays, $CD4^+$ memory ($CD4^+CD8^-CD45RO^+$) T cells were isolated from fresh PBMC using fluorescence-activated cell sorting. Migration assays were performed as previously described [38]. In brief, the human brain endothelial cell (EC) line hCMEC/D3 was obtained at Tebubio (Le Parray-en-Yvelines) and cultured in collagen-coated (rat tail, type I; Sigma-Aldrich) culture flasks in growth medium (EGM-2 MV medium (Lonza) supplemented with 2.5% FBS (Gibco, Thermo Fisher Scientific). For migration assays, hCMEC/D3 were trypsinized and cultured in Thincerts (24 well, translucent, 3 μm, Greiner Bio-One) at a density of 25×10^3 cells/cm^2. On day 3 and 5, hCMEC/D3 were replenished with EBM2 medium (Lonza) supplemented with 10 μg/mL gentamicin, 1 μg/mL amphotericin B, 1 ng/mL fibroblast growth factor, 1.4 μM hydrocortisone (all Sigma-Aldrich), and 2.5% FBS. On day 6, hCMEC/D3 were replenished with reduced medium supplemented with 10 μg/mL gentamicin, 1 μg/mL amphotericin B, 1 ng/mL fibroblast growth factor (all Sigma-Aldrich), and 0.25% FBS. Cultured barriers were left untreated (referred to hereafter as noninflamed) or treated with TNF-α (100 ng/mL, Peprotech) for 24 h (referred to hereafter as inflamed). Before adding the T cells, hCMEC/D3 cells grown on the inserts were washed with reduced medium and inserts were transferred to a new plate with fresh reduced medium. Sorted memory $CD4^+$ T cells (5×10^5 per insert, three inserts per condition) were allowed to migrate for 24 h. After migration, T cells from the well (migrated) and from the insert (non-migrated) were collected, counted, and used for flow cytometric analyses.

Results

Proportions of blood $Runx3^+$ and $Eomes^+$ memory $CD4^+$ T cells are decreased and targeted by NTZ in MS

First, we investigated the proportions of ($CD45RA^-$, central and effector) memory $CD4^+$ T cells expressing cytotoxicity-associated transcription factors Runx3, Eomes, and T-bet in the blood of healthy controls (HC, $n = 8$), treatment-naïve relapsing-remitting MS patients (MS, $n = 17$) and clinically stable MS patients treated with NTZ (NTZ-MS, $n = 8$). Compared with the HC group, the percentages of $Runx3^+$ and $Eomes^+$, but not $T\text{-}bet^+$ cells within the memory $CD4^+$ T-cell pool were significantly reduced in the MS group, which was not seen in the NTZ-MS

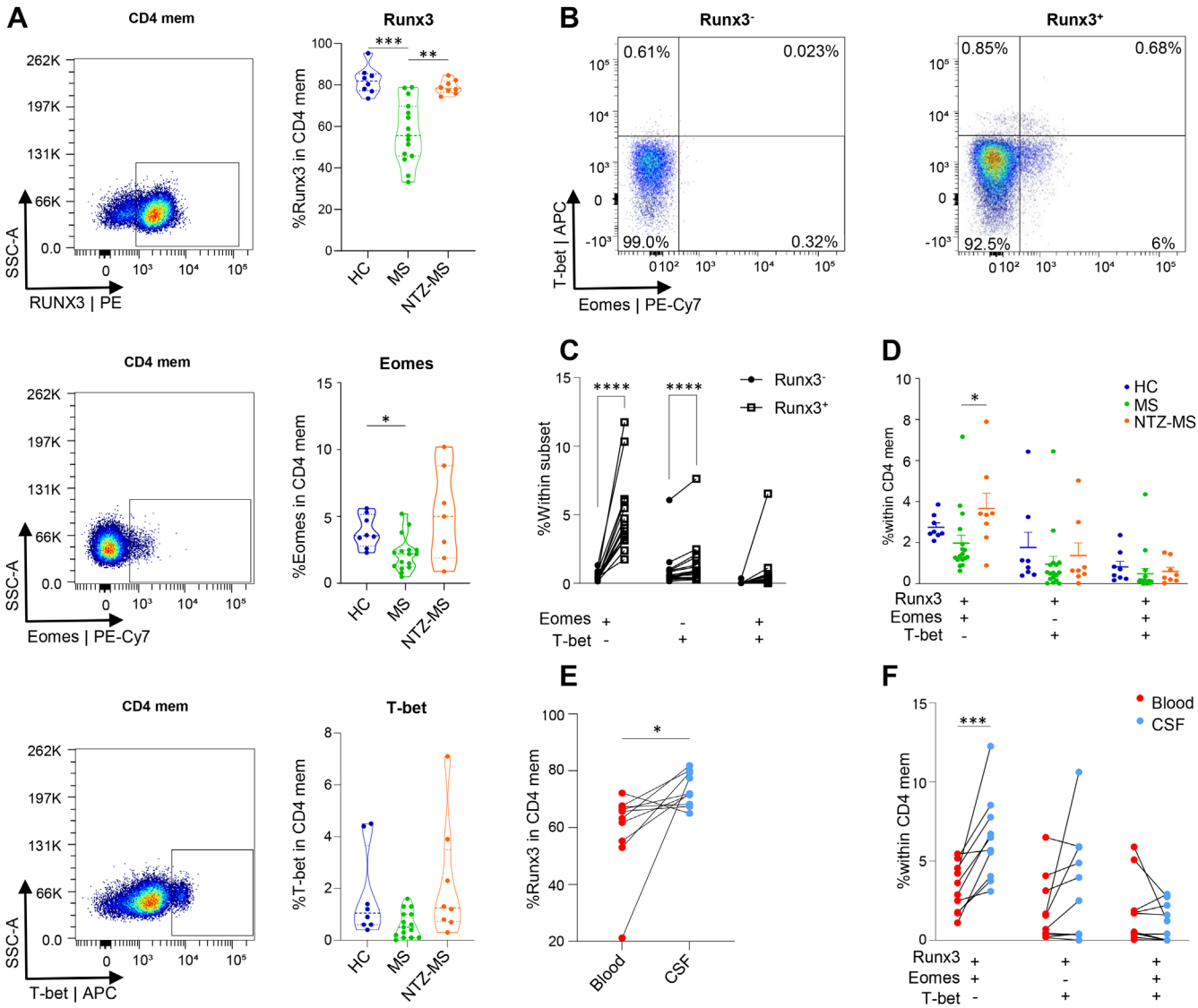

Figure 1. Relative frequencies of Runx3$^-$, Eomes$^-$, and/or T-bet$^-$ expressing CD4$^+$ memory T cells in MS blood and CSF. (A) Representative flow cytometry plots of TF Runx3, Eomes, and T-bet and expression of TF Runx3, Eomes, and T-bet are measured within CD4$^+$CD45RA$^-$ T cells (memory CD4$^+$ T cells) from healthy controls (HC, $n = 8$, blue dots), treatment-naive patients (MS, $n = 15$, green dots), and MS patients treated with natalizumab (NTZ-MS, $n = 8$, orange dots). Data were analyzed with one-way ANOVA, post hoc Tukey. Each violin plot shows median, quartiles, and range, and data were pooled from four independent experiments performed on thawed cells. (B) Representative flow cytometry plots (MS) and (C) cumulative data of co-expression of Runx3$^+$ vs. Runx3$^-$ with Eomes and T-bet within CD4$^+$ CD45RA$^-$ Th cells from MS donors ($n = 17$). Data were analyzed with two-way ANOVA, post hoc Tukey and were pooled from two independent experiments performed on thawed cells. (D) Cumulative data of co-expression of Runx3$^+$ with Eomes and T-bet within CD4$^+$ CD45RA$^-$ Th cells. Data shown is from HC ($n = 8$, blue dots), MS, ($n = 15$, green dots), and NTZ-MS ($n = 8$, orange dots). Data were analyzed with two-way ANOVA, post hoc Tukey. Graph shows mean ± SD, and data were pooled from four independent experiments performed on thawed cells. (E) Percentage of CD4$^+$ CD45RA$^-$ Runx3$^+$ in peripheral blood (red dots) versus cerebral spinal fluid (CSF; blue dots) from MS patients ($n = 10$). Data were analyzed with Wilcoxon tests. (F) Co-expression of Runx3, Eomes, and T-bet in memory Th cells isolated from peripheral blood and CSF from MS patients ($n = 10$). Data were analyzed with Wilcoxon tests. Data from panels (E) and (F) were pooled from 10 independent experiments and performed on fresh cells. *$P \leq 0.05$, **$P \leq 0.01$, ***$P \leq 0.001$, ****$P \leq 0.0001$.

group (Fig. 1A). Moreover, we found a significant enrichment of Eomes or T-bet expression in Runx3$^+$ as compared with Runx3$^-$ memory CD4$^+$ T cells (Fig. 1B,C). When analyzing co-expression patterns, the proportion of Runx3$^+$Eomes$^+$T-bet$^-$ cells was found to be significantly enriched in the NTZ-MS versus the MS group (Fig. 1D). These observations suggest recruitment of these cells to the inflamed CNS, which is inhibited by NTZ treatment. In line with these findings, Runx3$^+$ memory CD4$^+$ T cells were significantly enriched within the CSF of MS patients compared with paired blood samples (Fig. 1E). Upon further analysis, this enrichment was mainly driven by the Runx3$^+$Eomes$^+$T-bet$^-$ subset (Fig. 1F). Our data implicate that particularly Runx3 and Eomes co-expressing memory CD4$^+$ T cells are recruited to the CNS of treatment-naive MS patients.

Ex vivo Runx3$^+$Eomes$^+$T-bet$^-$ memory CD4$^+$ T cells preferentially express GZMK and not GZMB or PRF1

Co-expression of Runx3 with Eomes and/or T-bet is associated with the acquisition of a specific effector phenotype in memory CD4$^+$ T cells [34]. Therefore, we determined the *ex vivo* protein expression of GZMK, GZMB, and perforin (PRF1) in relation to these transcription factors to determine if this is indeed the case for Runx3$^+$ memory CD4$^+$ T cells (Fig. 2). Unsupervised clustering of high-parameter flow cytometry data, based on the median fluorescent intensity of the displayed markers, showed subclusters of cells with distinct expression profiles within the circulating CD4$^+$ Th pool of untreated MS patients. Runx3$^+$ clusters were associated with higher expression of GZMK, GMZB, and/or PRF1 compared with negative clusters (Fig. 2A). Within this subset, Runx3$^+$T-bet$^+$Eomes$^-$ clusters were characterized by high GZMB and variable PRF1 expression, whereas Runx3$^+$T-bet$^-$Eomes$^+$ clusters showed high GZMK expression. The Runx3 single-positive clusters showed relatively low expression of GZMK, GMZB, and PRF1. When using manual gating to determine the percentage of cells that were considered positive for a selected marker, GZMK was indeed expressed by Runx3$^+$Eomes$^+$T-bet$^-$ memory CD4$^+$ T cells (Fig. 2B). GZMB expression did not significantly associate with one of the transcription factor profiles (Fig. 2C). PRF1 expression was highest in Runx3$^+$Eomes$^{-/+}$T-bet$^+$ memory CD4$^+$ T cells (Fig. 2D). In accordance with the enrichment of Runx3$^+$Eomes$^+$T-bet$^-$ cells in the memory CD4$^+$ T-cell pool, we found that the percentage of memory CD4$^+$ T cells expressing GZMK was significantly increased within the CSF compared with blood of treatment-naive MS patients (Fig. 2B), whilst the expression of PRF1 and GZMB was unchanged (Fig. 2C,D). These findings could imply that Runx3$^+$Eomes$^+$T-bet$^-$ memory CD4$^+$ T cells are preferentially recruited to the CSF of MS patients by increased production of GZMK.

The Th17.1 subset is enriched for Runx3$^+$Eomes$^+$T-bet$^-$ and characterized by CCR5^{high} and GZMK$^+$ cells

To gain more insight into the effector phenotype of such memory CD4$^+$ T cells, we next explored associations between transcription factor expression and chemokine receptor profiles *ex vivo* in treatment-naïve MS patients (Fig. 3). Aside from the classical Th-associated chemokine receptors (CCR6, CXCR3, and CCR4), CCR5 expression was of special interest since it was recently shown that CCR5^{high} expressing memory CD4$^+$ T cells are able to infiltrate the CNS via GZMK-mediated trans-endothelial diapedesis [40]. We found that Runx3 single-expressing memory CD4$^+$ T cells showed high expression of CCR6 and CCR4, whereas CCR4 levels were reduced and CXCR3 was more upregulated on Runx3 and Eomes co-expressing subsets (Fig. 3A–C). T-bet-expressing subsets showed the lowest CCR6 and CCR4 levels. When defining the expression of CCR5 as either dim or high (Fig. 3D, left), it was found that CCR5^{dim} cells were enriched within Runx3$^+$ memory CD4$^+$ T cells that expressed T-bet either alone or with Eomes (Fig. 3D, middle). Runx3 and Eomes but not T-bet expression were associated with an increased percentage of memory CD4$^+$ cells that displayed high levels of CCR5 (Fig. 3D, right). Accordingly, high CCR5 levels coincided with increased expression of GZMK, which was not seen for GZMB and PRF1 (Fig. 3E). Collectively, these results indicate that a Runx3$^+$Eomes$^+$T-bet$^-$ phenotype characterizes memory CD4$^+$ T cells with high levels of brain-homing markers CCR5 and GZMK.

Besides analyzing the expression levels of individual chemokine receptors, memory CD4$^+$ T cells can be subdivided into distinct proinflammatory subsets based on CCR6, CXCR3, and CCR4 expression patterns [13]. Using the gating strategy as depicted in Fig. 4A, we next analyzed Runx3, Eomes, and T-bet expression in blood Th1 (CCR6$^-$CXCR3$^+$CCR4$^-$), Th17 (CCR6$^+$CXCR3$^-$CCR4$^+$), Th17 double-positive (DP; CCR6$^+$CXCR3$^+$CCR4$^+$), and Th17.1 (CCR6$^+$CXCR3$^+$CCR4$^{-/dim}$) cells. Th1 and Th17.1 cells exhibited the highest proportions of Runx3$^+$ cells (Fig. 4B). In contrast to other subsets, the Eomes$^+$T-bet$^-$ fraction was specifically enriched in Runx3$^+$ Th17.1, while this was the case for both Eomes$^+$T-bet$^-$ and Eomes$^+$T-bet$^+$ fractions in Runx3$^+$ Th1 cells (Fig. 4C). In accordance with the earlier characteristics associated with these transcription factor expression profiles, Th1 and Th17.1, and to a lesser extent Th17DP cells, showed increased expression of GMZK (Fig. 4D). Moreover, the Th1 subset was enriched for GZMB- as well as PRF1-expressing cells. Notably, Th17.1 cells showed the highest CCR5 expression (Fig. 4E), which was consistent with its selective enrichment for Runx3$^+$Eomes$^+$T-bet$^-$ (Fig. 4C) and related expression levels of GZMK (Fig. 3E). Taken together, our results demonstrate that the Runx3$^+$Eomes$^+$T-bet$^-$, CCR5^{high}, and GZMK^{high} phenotype of memory CD4$^+$ T cells mainly corresponds to the Th17.1 subset.

Th17.1 differ from CD4$^+$CD28$^-$ T cells and selectively migrate across a noninflamed BBB *in vitro*

The acquisition of cytotoxic features in memory CD4$^+$ T cells is commonly associated with a loss of CD28 expression in Th1-skewed cells [12]. Because Th17.1 cells also possess Th1-related features, we assessed the extent to which the identified effector phenotypes overlapped between CD4$^+$CD28$^-$ T cells and Th17.1 cells. In our MS cohort, CD4$^+$CD28$^-$ memory T cells (see Fig. 5A) exhibited lower expression of CCR6, CCR4, and CXCR3 compared with their CD28$^+$ counterparts (Fig. 5B). Accordingly, among all Th subsets analyzed, CD28$^-$ fractions were predominant in Th1 and hardly found in Th17.1 cells (Fig. 5C). Runx3 levels were not significantly different between memory CD4$^+$CD28$^-$ and CD28$^+$ T cells (Fig. 5D). In comparison with Th17.1 (Fig. 4C), the memory CD4$^+$CD28$^-$ population was enriched for Runx3$^+$Eomes$^-$T-bet$^+$ cells (Fig. 5E) and showed lower frequencies of CCR5^{high} cells (Fig. 5F). To be able to assess intracellular GZMK, GZMB,

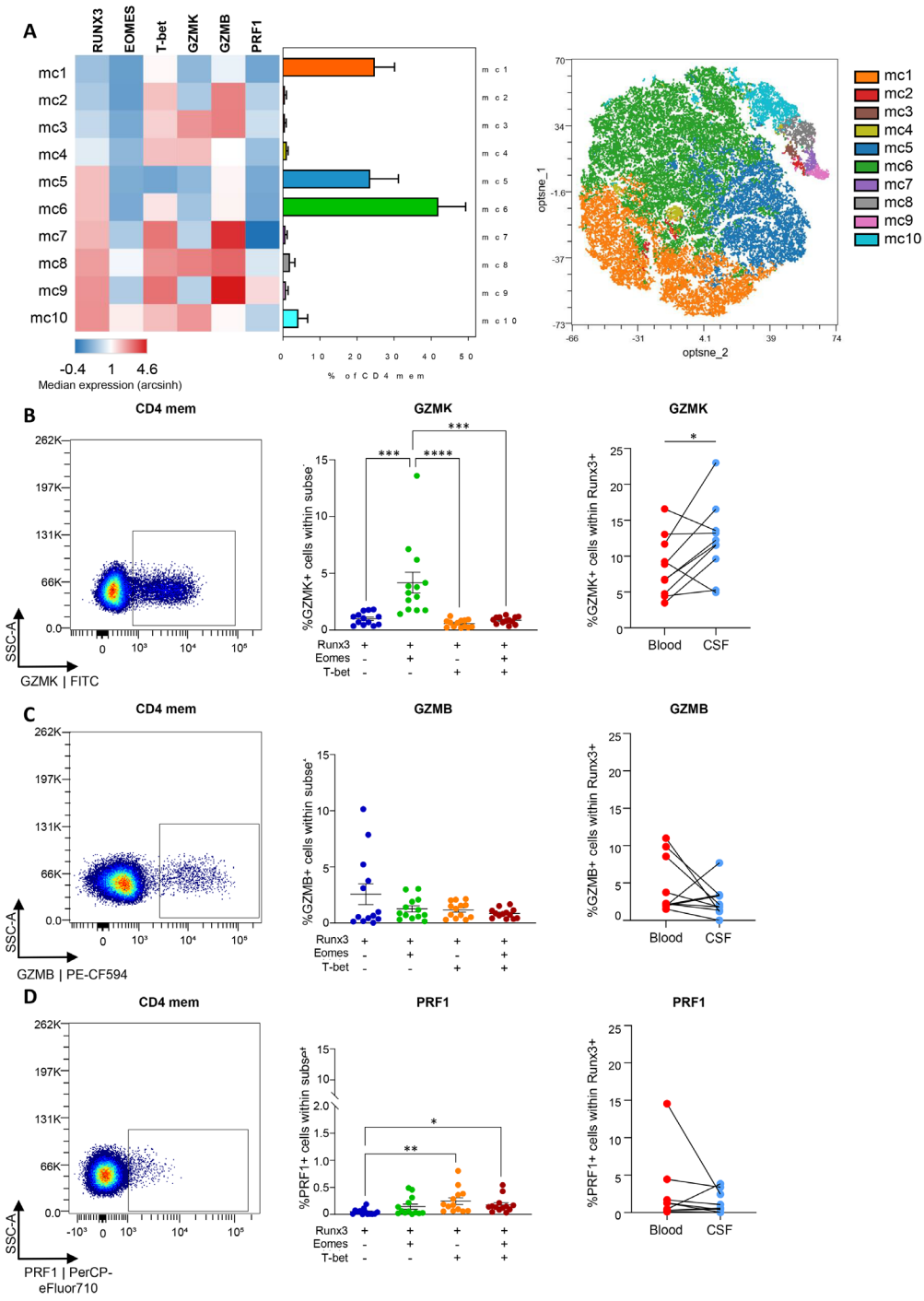

Figure 2. GZMK-expressing memory CD4$^+$ T cells are characterized by co-expression of Runx3 and Eomes, and are enriched in the CSF of treatment-naïve MS patients. (A) Flow cytometry data of treatment-naïve MS (n = 14) were analyzed using the unsupervised automated clustering tool FlowSOM [39] which utilizes median fluorescence intensity of given markers to compare protein expression between cell populations. Live, single CD3$^+$CD8$^-$CD45RA$^-$ cells were categorized into 10 metaclusters (mc) based on their expression of TF (Runx3, Eomes, T-bet) and cytolytic molecules (GZMB, GZMK, PRF1). The median fluorescence intensity (arcsinh-transformed) of each marker within the metaclusters is displayed in the heatmap (left), as well as abundance of each metacluster within the memory CD4$^+$ T cell population (middle). Mutual phenotypic resemblance of metaclusters is visualized using a dimensionality reduction approach with the opt-SNE algorithm and overlay of FlowSOM metaclusters (right). Data were pooled from two independent experiments performed on thawed cells. (B–D) Representative flow cytometry plots (left), subpopulations based on TF co-expression profiles expressing cytolytic molecules (MS, n = 13; middle), cytolytic molecule expression in blood versus CSF (MS, n = 10; right) of GZMK (B), GZMB (C), PRF1 (D). Data were analyzed using the Kruskal–Wallis test, post hoc Dunn or Wilcoxon test. Figures in the middle panel show mean ± SD with data pooled from two independent experiments performed on thawed cells. Data shown in the right panel was pooled from 10 independent experiments performed on fresh cells. Samples with <100 events within the analyzed gate were excluded from analysis to ensure high-quality data. *P ≤ 0.05, **P ≤ 0.01, ***P ≤ 0.001, ****P ≤ 0.0001.

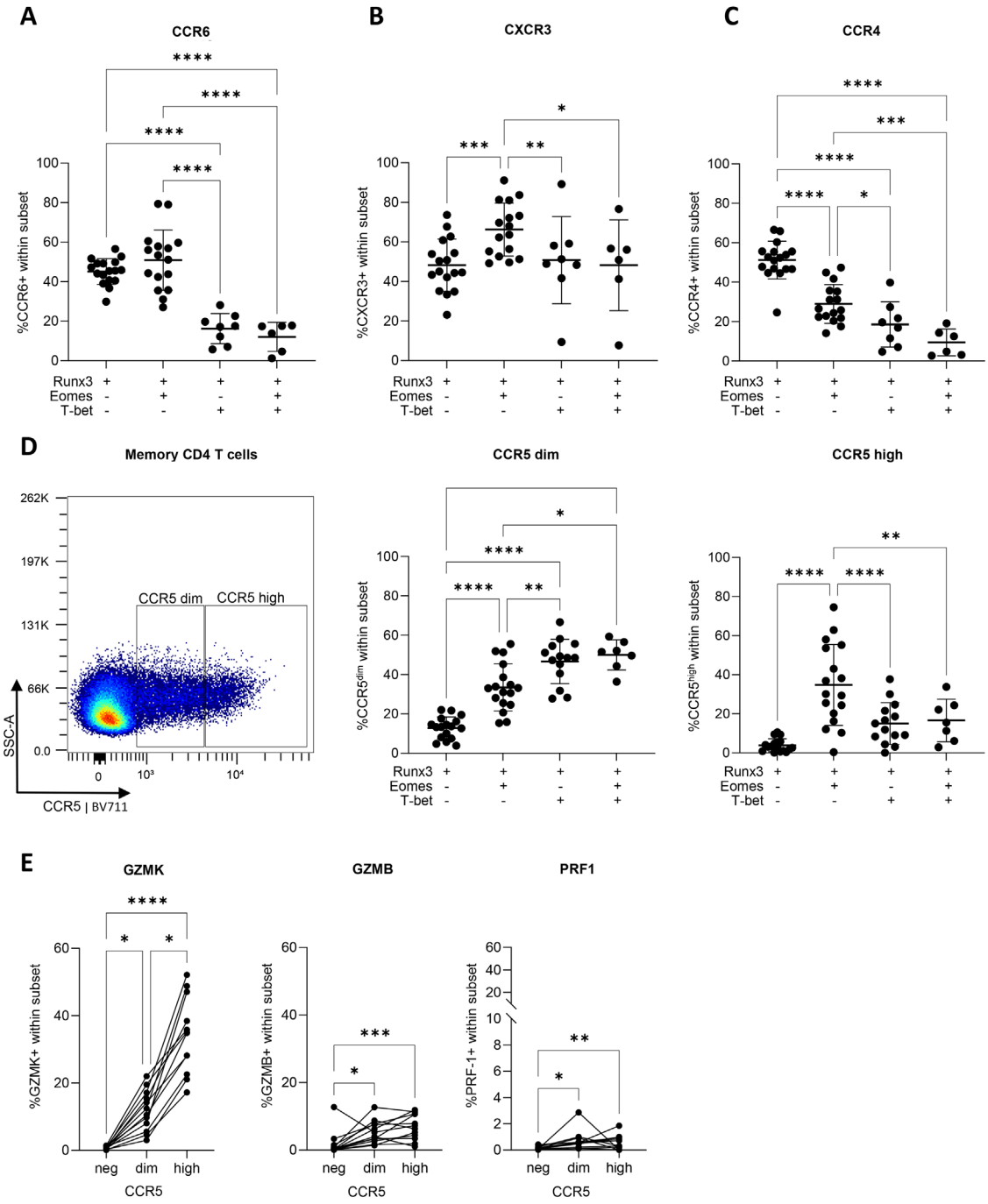

Figure 3. Runx3$^+$ Eomes$^+$ Tbet$^-$ CD4 T-memory cells express high CCR6, CXCR3, dim CCR4 high CCR5. (A–D) Percentage of memory CD4$^+$ T cells expressing CCR6 (A), CXCR3 (B), and CCR4 (C). within the previously described TF profiles. Figures show mean ± SD. Data were analyzed with a two-way ANOVA, post hoc Tukey. (D) Representative dotplot of CCR5^{dim} and CCR5^{high} gating. (E) Association of CCR5 expression with either GZMK, GZMB, or PRF1 expression. All data shown is generated from PBMCs of treatment-naïve MS patients pooled from two independent experiments (n = 17) performed on thawed cells. Samples with <100 events within the analyzed gate were excluded from analysis to ensure high-quality data. Data were analyzed with Friedman test, post hoc Dunn. *$P \leq 0.05$, **$P \leq 0.01$, ***$P \leq 0.001$, ****$P \leq 0.0001$.

and PRF1 expression in memory CD4$^+$CD28$^-$ T cells, we used blood samples from CMV-seropositive blood donors, allowing for analysis of sufficient numbers of CD4$^+$CD28$^-$ cells [41] (Fig. 5G). GZMB and PRF1 but not GZMK were highly expressed in memory CD4$^+$CD28$^-$ versus CD28$^+$ T cells (Fig. 5H), further supporting our observation that Th17.1 and CD4$^+$CD28$^-$ T cells are subsets with a distinct effector phenotype.

Lastly, we explored the association of these *ex vivo* characteristics with the ability of memory CD4$^+$ T-cell subsets to cross BBB-derived EC layers *in vitro*. We used both noninflamed (left)

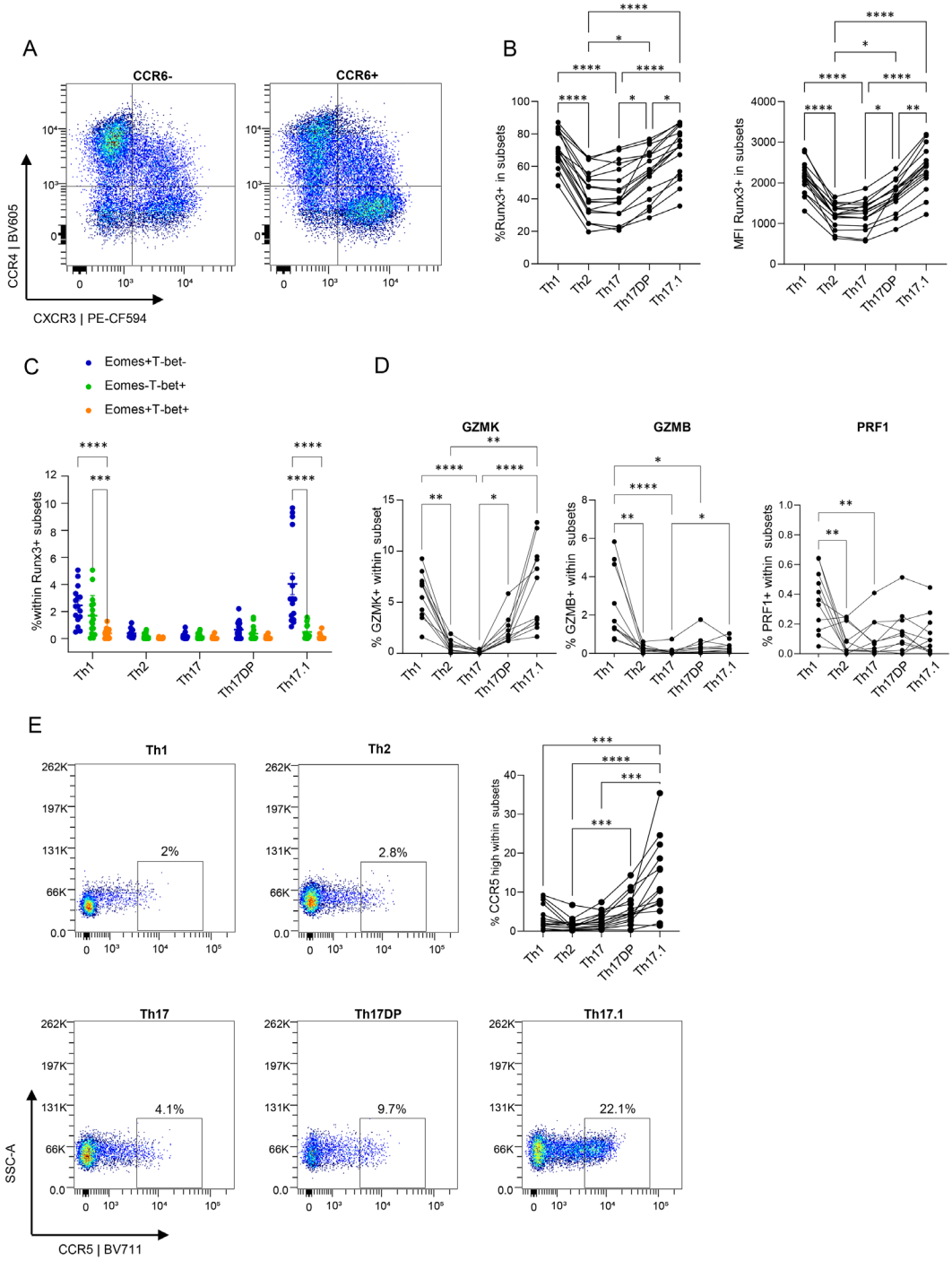

Figure 4. The Th17.1 subset predominantly co-expresses Runx3 and Eomes and consists of high frequencies of GZMK^{+} and CCR5^{high} cells. (A) Representative dotplots of gating Th1, Th2, Th17, Th17DP, and Th17.1 subsets within the single, live CD4^{+}CD45RA^{-} population, using co-expression of CCR6, CCR4, and CXCR3. (B) Expression level of Runx3 (left; expressed as percentage, right; expressed as median fluorescence intensity (MFI) within memory Th subsets. Data were analyzed with Friedman test, post hoc Dunn. Data shown were obtained using PBMC isolated from treatment-naïve MS patients (n = 17) measured in two independent experiments. (C) Co-expression of Eomes and T-bet within Runx3-expressing memory Th subsets. Data were analyzed with two-way ANOVA, post hoc Tukey. This figure shows the mean ± SD. Data shown were obtained using PBMC isolated from treatment-naïve MS patients (n = 17) measured in two independent experiments. (D) Expression of GZMK, GZMB, and PRF1 within memory CD4^{+} T subsets. Data were analyzed with two-way ANOVA, post hoc Tukey. Data shown were obtained using PBMC isolated from treatment-naïve MS patients (n = 13) measured in two independent experiments. (E) Representative dotplots of CCR5^{high} gating in Th1, Th2, Th17, Th17DP, and Th17.1 and quantification of percentage CCR5^{high} within memory CD4^{+} T subsets. All data shown were obtained using PBMC isolated from treatment-naïve MS patients (n = 17) measured in two independent experiments. Data shown were obtained using PBMC isolated from treatment-naïve MS patients (n = 16) measured in two independent experiments. All data samples with <100 events within the analyzed gate were excluded from analysis to ensure high-quality data. *P ≤ 0.05, **P ≤ 0.01, ***P ≤ 0.001, ****P ≤ 0.0001. All data shown were obtained using thawed cells.

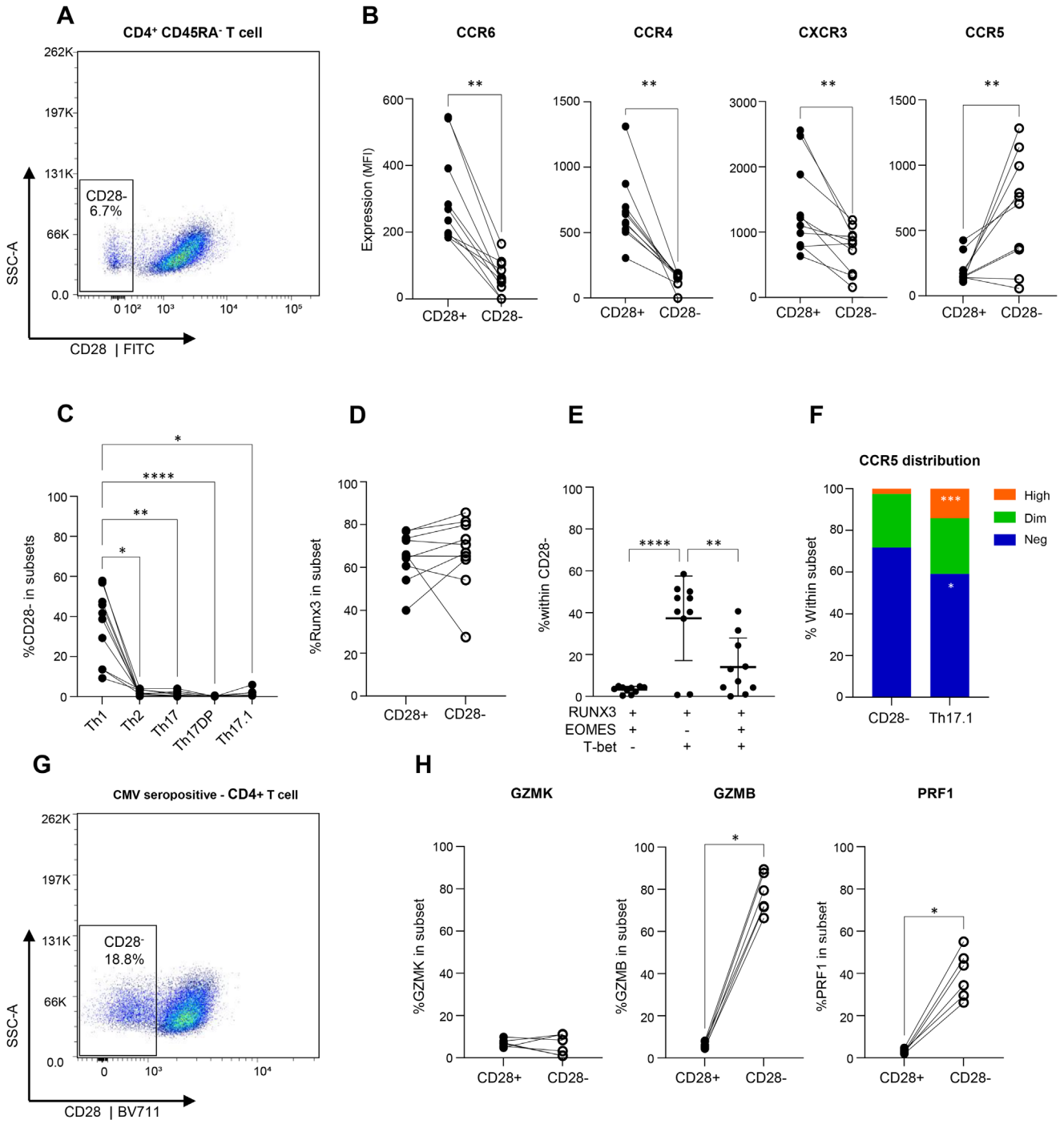

Figure 5. CD4⁺CD28⁻ memory cells show distinct expression of CNS homing-related transcription factors, chemokine receptors, and cytoxicity-associated molecules. (A) Representative dotplot of gating CD28⁻CD45RA$^{+/-}$ memory CD4⁺ T cells within the single, live CD4⁺ population, in the treatment-naïve MS cohort (n = 10; data displayed in panel B–F) and was pooled from two independent experiments. Data were analyzed with the Friedman test, post hoc Dunn. (B) Antigen density of chemokine receptors CCR6, CCR4, CXCR3, and CCR5. Data were analyzed with Wilcoxon tests. (C) Prevalence of CD28⁻ cells within memory Th subsets on the surface of CD28⁺ and CD28⁻ memory CD4⁺ T cells. Data were analyzed with Wilcoxon test. (D) Expression of Runx3 within CD28⁺ and CD28⁻ memory CD4⁺ T. Data were analyzed with Wilcoxon tests. (E) Co-expression of Eomes and T-bet within Runx3-expressing CD28⁻ memory CD4⁺ T Th cells. Data were analyzed with two-way ANOVA, post hoc Tukey. This figure shows the mean ± SD. (F) CCR5 population distribution CD28⁻ and Th17.1. All previously shown data were measured in two independent experiments. (G) Representative dotplot of gating CD28⁻CD45RA$^{+/-}$ memory CD4⁺ T cells within the single, live CD4⁺ population, in the cytomegalovirus (CMV)-seropositive HC cohort (n = 6; data displayed in panel G, H). Shown data are from one experiment. (H) Expression of GZMK, GZMB, and PRF1 within CD28⁺ and CD28⁻ memory CD4⁺ T subsets. Data were analyzed with Wilcoxon tests. *P ≤ 0.05, **P ≤ 0.01, ***P ≤ 0.001, ****P ≤ 0.0001. All data shown were obtained using thawed cells.

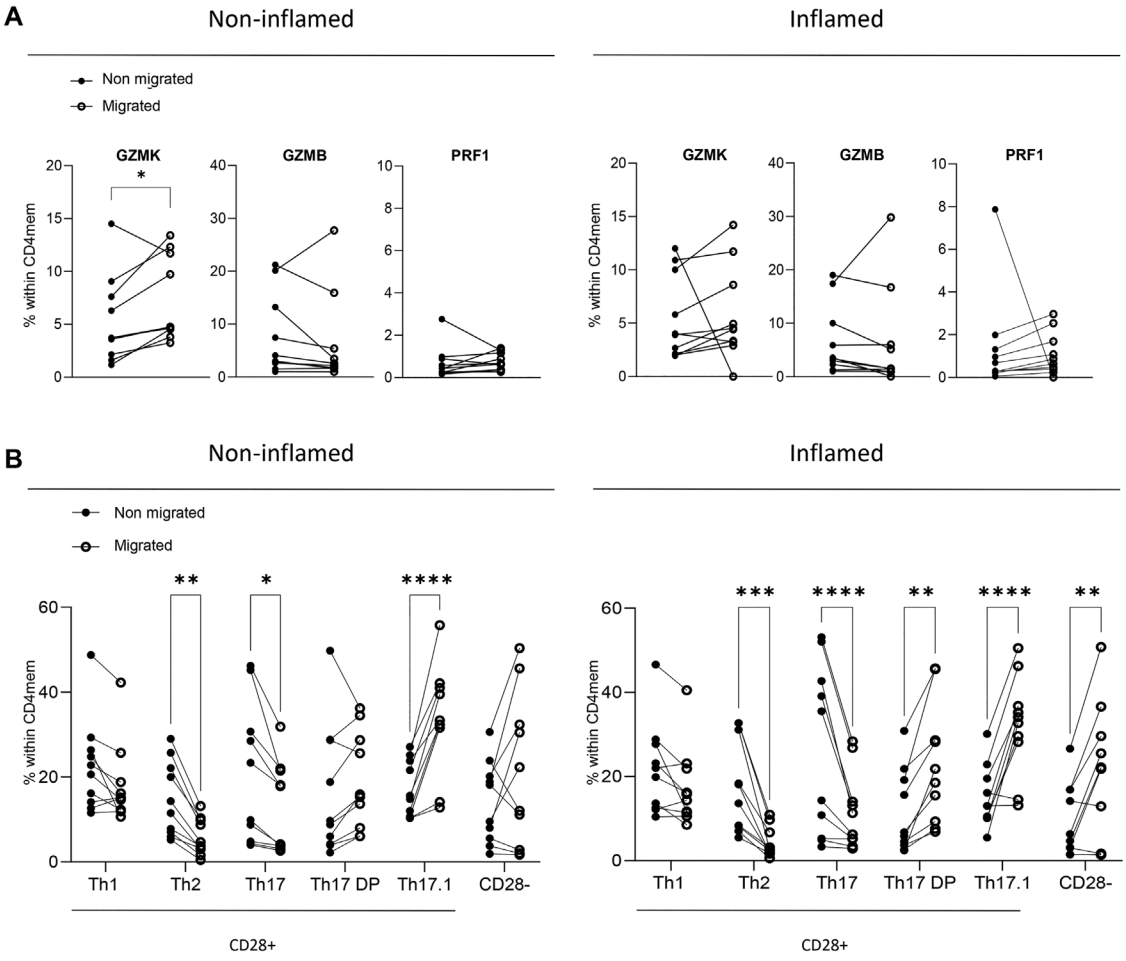

Figure 6. Different capacities of MS-associated CD4$^+$ memory T cells to cross noninflamed and inflamed BBB *in vitro*. For the migration assay fresh FACS-sorted memory CD4$^+$ T cells isolated from HC (n = 10) were placed on top of a transwell insert with a confluent monolayer of hCMEC/d3 cells (EC). EC were either inflamed with TNF-α for 24 h prior to migration (referred to as "inflamed"), or left untouched (referred to as "non-inflamed"), as described previously [38]. Memory CD4$^+$ T cells were allowed to migrate for 24 h, after which the cells present in the transwell insert and cells in the bottom well were collected for flow cytometry analyses. Th subsets were phenotyped using the gating strategy depicted in Fig. S1; Th1 cells were gated within the CD28$^+$ population. (A) GZMK, GZMB, and PRF1 expression in total CD4$^+$ memory population following *in vitro* migration. (B) The phenotype distribution in memory CD4$^+$ T cells was analyzed following *in vitro* migration. Data were analyzed with two-way ANOVA, post hoc Bonferroni. Data were pooled from seven independent experiments. $^*P \leq 0.05$, $^{**}P \leq 0.01$, $^{***}P \leq 0.001$, $^{****}P \leq 0.0001$.

and inflamed (right) EC layers to address if preactivation of the BBB is a determinant for their migratory capacity [42]. In CD4$^+$ T-cell fractions that crossed noninflamed EC layers, proportions of GZMK- and not GZMB- and PRF1-positive cells were enriched as compared with nonmigrated fractions (Fig. 6A, left). Under inflamed conditions, no significant enrichment of any of these cells was found (Fig. 6A, right). In addition, when using noninflamed layers, Th17.1 was the only subset to be enriched in the migrated versus the nonmigrated fraction (Fig. 6B, left). This was less selective and accounted for Th17.1, Th17DP, and CD28$^-$ subsets when using inflamed layers (Fig. 6B, right). These data show that Th17.1 and CD4$^+$CD28$^-$ memory T cells not only show a difference in effector phenotype but also in their ability to migrate through the BBB. Moreover, within the memory CD4$^+$ T-cell pool, GZMK-expressing Th17.1 cells may be the first in activating and crossing a noninflamed human BBB.

Discussion

Some of the pivotal players in MS disease progression are believed to be CNS-infiltrating memory CD4$^+$ T cells [43, 44]. Although Eomes-expressing migratory CD4$^+$ T cells have been described before in the context of progressive MS [45], it remains unknown if and how effector phenotypes differ between subsets that have previously been identified as pathogenic in MS, and to what degree this amounts to the different aspects of MS pathology. The aim of this study was to confirm and expand on this knowledge by more broadly investigating the features of human memory CD4$^+$ T cells that are prone to enter the CNS in MS and validate their CNS-homing potential in both *ex vivo* and *in vitro*. Here, we showed that the proportions of memory CD4$^+$ T cells expressing Runx3 and Eomes were decreased in the circulation of MS patients. This finding was supported by an enrichment of

Runx3$^+$Eomes$^+$T-bet$^-$ cells in the CSF, whereas their presence in the circulation was restored following NTZ treatment. Furthermore, we found that co-expression of Runx3 and Eomes together with a lack of T-bet defined memory CD4$^+$ T cells with elevated levels of CCR6, CXCR3, CCR5, and GZMK, an effector phenotype corresponding to Th17.1. This was different compared with another MS-associated subset, defined as CD4$^+$CD28$^-$ T cells, which displayed a Runx3$^+$Eomes$^-$T-bet$^+$ profile with intermediate expression of CCR5 as well as expression of GZMB and PRF1. When assessing the brain-homing potential of CD4$^+$ T-cell subsets *in vitro*, Th17.1 cells were selectively capable of crossing a BBB-derived EC layer under noninflamed conditions. Other pathogenic subsets, including CD4$^+$CD28$^-$ cells, showed enhanced transmigration when using inflamed barriers. Hence, memory CD4$^+$ T cells contain small fractions with distinct effector phenotypes that likely define their ability to enter the CNS during the MS course.

As NTZ is a monoclonal antibody against VLA-4 that traps CNS-infiltrating T cells within the circulation [46, 47], blood samples of NTZ-treated MS patients represent an ideal and accessible source to study the CNS-homing features of subsets during the relapsing-remitting phase of the disease. We have previously validated this approach for brain-homing CD4$^+$ T cells [13], CD8$^+$ T cells [48], and B cells [49]. Besides preventing their entry into the CNS, NTZ treatment has also been shown to induce phenotypical changes in memory CD4$^+$ T cells, including acquisition of a detrimental effector phenotype that may at least partly be responsible for severe disease rebounds experienced by some NTZ-treated MS patients [50, 51]. This could be an alternative explanation for the increased percentage of circulating Runx3$^+$ and Eomes$^+$ memory CD4$^+$ T cells observed in the NTZ-treated compared with treatment-naive MS patients. However, the fact that the presence of these subsets was not different between NTZ-MS and HC blood and was enriched in CSF suggests that both Runx3 and Eomes are involved in a selective CNS-homing ability of CD4$^+$ T cells in MS. Although proof is lacking, this may be differentially regulated during the MS course, as others have shown that CD4$^+$ T cells expressing Eomes are elevated in both blood and CSF of secondary progressive MS versus relapsing-remitting MS and healthy control groups [45, 52].

Previously, it was shown that Runx3 regulates the expression of both Eomes and T-bet in cytotoxic T cells [53]. The relative expression levels of Eomes and T-bet are known to be important determinants of effector phenotypes, including those of CD4$^+$ T cells. Work by others has shown that three distinct effector populations can be identified based on the expression of Eomes and T-bet. In mice, Eomes$^+$T-bet$^-$ T cells exhibited robust cytotoxic activity, whereas Eomes$^-$T-bet$^+$ counterparts were exclusively Th1 with a more intermediate cytotoxic phenotype [54]. However, another study found that during *in vitro* differentiation of human CD4$^+$ T cells, Eomes appeared to be redundant for the acquisition of GZMB and PRF1, whereas T-bet was necessary to develop these features [34]. These types of CD4$^+$ T cells were found to be predominantly Th1-like, which is consistent with our findings for CD4$^+$CD28$^-$ T cells. This suggests that following Runx3 upregulation, Eomes regulates the differentiation of noncytotoxic, whereas T-bet regulates the differentiation of cytotoxic Th1-like cells in humans. In line with this notion, unsupervised clustering of high-parameter flow cytometry data revealed separate subsets of circulating Runx3$^+$ memory CD4$^+$ T cells co-expressing Eomes and GMZK and co-expressing T-bet and GZMB with and without PRF1. It should be noted however that the absolute percentage of CD4$^+$ memory cells expressing PRF1 remains low. Overall, our results are in accordance with effector features of cytotoxic-like CD4$^+$ T-cell subsets described in a recent single-ell RNA analysis study using CSF-derived immune cells of MS patients [55].

Although this study focuses on analyzing the *ex vivo* effector phenotype of circulating and CSF-derived CD4$^+$ memory T cells at protein level, the effector functions that contribute to MS pathology remain to be determined for the subsets described here. Nonetheless, a previous study identified a subset of human CD4$^+$ T cells with enhanced cytolytic potential, showing low T-bet and high Eomes and GZMK expression [56]. Following infiltration into the CNS, additional expression of cytotoxic molecules GMZB and PRF1 in memory CD4$^+$ T cells may potentially lead to oligodendrocyte loss and axonal injury as suggested by the co-localization of memory CD4$^+$ and CD8$^+$ T cells with affected CNS-resident cells in other studies [25, 57, 58]. *In vitro* killing of human oligodendrocytes [29] and ECs [59] by T-cells expressing GZMB and PRF1 further illustrate mechanisms by which these types of subsets can exacerbate MS. In addition, the possibility that increased expression of effector molecules is a transient effect mediated by interaction with the BBB, which has been described for murine Tregs [60, 61] and human monocytes [62], was not explored here but poses an interesting area of research for further studies.

Runx3 and Eomes co-expressing cells were solely enriched in Th17.1 (CCR6$^+$CXCR3$^+$CCR4$^{-/dim}$), a memory CD4$^+$ T cell that is associated with MS manifestation [13]. This Runx3$^+$Eomes$^+$T-bet$^-$ phenotype corresponded to high CCR5 and GZMK expression. Interestingly, GZMK has previously been described to have a noncytotoxic intra- and extracellular role including endothelial activation [63]. In line with this, Herich et al. [40] have shown that human CCR5^{high} effector memory CD4$^+$ T cells cross the BBB via GZMK-mediated trans-endothelial diapedesis. These CCR5^{high} cells use their high levels of VLA-4 to arrest scattered VCAM-1 on the BBB. Subsequently, CCR5^{high} cells release GZMK to upregulate ICAM-1 on the EC layer, which is recognized by LFA-1 on the T cell to enable extravasation. Preferential migration of GZMK$^+$ CD4$^+$ T cells was confirmed in our *in vitro* transmigration assay. Given our current findings on CCR5 and GZMK expression within the Th17.1 subset and our previous findings that Th17.1 expresses high levels of VLA-4 [13], we hypothesize that Th17.1 uses a similar mechanism to infiltrate into the CNS in MS. This process may be facilitated by other effector mechanisms described for the same types of CD4$^+$ T cells [64]. In our hands, only Th17.1 cells showed an enhanced potential to cross a noninflamed BBB *in vitro*. Therefore, due to Runx3- and mainly Eomes-induced upregulation of GZMK and corresponding activation of the BBB, Th17.1 may represent a subset that paves the way for other immune cells to infiltrate the CNS.

Based on their *ex vivo* effector phenotypes, Th17.1 and $CD4^+CD28^-$ T cells represent two different subsets, albeit skewing toward similar, cytotoxic-like cells under certain (local) inflammatory conditions cannot be ruled out and is still well possible. In MS patients, memory $CD4^+CD28^-$ T-cell proportions are increased in the blood, which is associated with a faster disease progression. Furthermore, these cells have the capacity to enter inflammatory sites and accumulate in MS brain lesions [21, 24–26]. Upon activation, they produce IFN-γ [65] and GM-CSF but lack expression of IL-17 [66]. They mediate their cytotoxic potential through the expression of NK cell receptors and by directed exocytosis of cytotoxic granules. [25, 67]. Here, we showed that memory $CD4^+CD28^-$ T cells are enriched for $Runx3^+Eomes^-T\text{-}bet^+$ subsets and confirmed that these cells expressed both GZMB and PRF1. These cells were most similar to Th1 cells with regards to chemokine receptor expression and exhibited an intermediate expression of CCR5. $CD4^+$ $CD28^-$ T cells only showed enhanced transmigration in our *in vitro* assay under inflamed conditions, which may imply that this subset depends on other cells that interact with the BBB such as Th17.1 (see above) for their entry into the CNS. The differences in chemokine receptor expression on $Eomes^+T\text{-}bet^-$ (Th17.1) and $Eomes^-T\text{-}bet^+$ ($CD28^-$) memory $CD4^+$ T cells additionally suggest that these subsets use different routes to enter the CNS. This is possibly explained by differential CCR6 expression, which mediates the transmigration of memory $CD4^+$ T cells via the blood–cerebrospinal fluid barrier at the choroid plexus [42, 68]. In our view, this should be addressed further using *in vitro* models of the blood–cerebrospinal fluid barrier. The reduced intensity of CCR6 and CXCR3 expression, coupled with the ability to migrate across an inflamed BBB *in vitro*, indicates that $CD4^+CD28^-$ T cells use other effector molecules during their migration process. This is in accordance with our previous findings that these cells express high levels of fractalkine receptor (CX3CR1) and utilize this molecule to reach the inflamed CNS [24]. A different approach in addressing functional responses of memory $CD4^+$ T cells in the context of MS was recently employed by Cruciani et al. [5] who looked into the specificity of CSF-infiltrating T cells against autoantigens implicated in MS. In patients with autoreactive T cells, they found an enrichment of $CD27^-CD28^+$ Th1 cells with overexpression of T-bet, Eomes, various granzymes, and IFN-γ as well as a lack of CCR6 and CCR4. Because loss of CD27 is indicative of a precursor population of cytotoxic $CD4^+$ T cells [69], this may represent a subset similar to $CD4^+CD28^-$ T cells, but in a less differentiated stage. Although their study uses an elegant approach to combine the functionality of memory $CD4^+$ T cells with deep immunophenotyping, it should be noted that only 14 out of 105 MS patients showed an IFN-γ-positive $CD4^+$ T-cell response to different epitopes of GDP-L-FS, of which four out of seven patients were enriched for $CD27^-CD28^+$ (Th1) cells [5]. Other work by the same group revealed that autoreactive (RASGRP2) IFN-γ-positive memory $CD4^+$ T cells mainly have a $CCR6^+CXCR3^+$ phenotype, also depending on the presence of HLA-DRB1*1501 [2]. The latter corresponds with our earlier findings [13, 28] and current work that Th17.1 cells ($CCR6^+CXCR3^+$) are more capable of entering the CNS in MS.

Taken together, we show here that expression of the transcription factors Runx3, Eomes, and T-bet subdivides memory $CD4^+$ T cells into subsets with distinctive brain-homing phenotypes. More specifically, Runx3 and Eomes co-expressing subsets that lack T-bet can be defined as being predominantly Th17.1 cells with high levels of CCR5 and GZMK. Runx3 and T-bet co-expressing subsets that lack Eomes appear to be primarily Th1 ($CD28^-$) cells, which express GZMB and PRF1. These findings shed light on the effector phenotype of human brain-homing $CD4^+$ T-cell subsets that are associated with MS and thereby provide a framework for the identification of new and highly specific therapeutic targets.

Acknowledgements: The hCMEC/D3 cell line was provided by Tebubio (Le Perray-en-Yvelines, France). This study was funded by the Dutch MS Research Foundation (19-1057 MS, 19-1075 MS, and 20-490f MS) and the Dutch Research Council (ZonMw-Vidi grant 09150171910036).

Conflict of interest statement: M.M.v.L. received research support from EMD Serono, Merck, GSK, and Idorsia Pharmaceuticals Ltd. J.S. received lecture and/or consultancy fees from Biogen, Merck, Novartis, Roche, and Sanofi-Genzyme. The remaining authors declare no conflict of interest.

Author contributions: Cindy Hoeks and Steven C. Koetzier contributed to experimental design and funding acquisition. Cindy Hoeks, Fabiënne van Puijfelik, and Steven C. Koetzier contributed to data generation, data analyses, and data interpretation. Cindy Hoeks and Fabiënne van Puijfelik wrote the manuscript. Marie-José Melief and Annet F. Wierenga-Wolf performed the experiments. Cato E.A. Corsten collected clinical data. Jasper Rip, Piet Stinissen, Joost Smolders, and Niels Hellings interpreted the results and critically revised the manuscript. Bieke Broux and Marvin M. van Luijn designed the research, interpreted the results, and critically revised the manuscript. All authors have read and agreed to the published version of the manuscript.

Ethics statement: The studies involving human participants were reviewed and approved by the Medical Ethics Committee Erasmus MC (MEC-2014-033).

Informed consent statement: The patients/participants provided their written informed consent to participate in this study.

Data availability statement: The data that support the findings of this study are available from the corresponding author upon reasonable request.

Peer review: The peer review history for this article is available at https://publons.com/publon/10.1002/eji.202350544

References

1 **Charabati, M., Zandee, S., Fournier, A. P., Tastet, O., Thai, K., Zaminpeyma, R., Lécuyer, M. A., et al.**, MCAM+ brain endothelial cells contribute to neuroinflammation by recruiting pathogenic CD4+ T lymphocytes. *Brain* 2023. **146**: 1483–1495.

2 **Jelcic, I., Al Nimer, F., Wang, J., Lentsch, V., Planas, R., Jelcic, I. Madjovski, A., et al.**, Memory B cells activate brain-homing, autoreactive CD4(+) T cells in multiple sclerosis. *Cell* 2018. **175**: 85–100 e23.

3 **Alvarez, J. I., Saint-Laurent, O., Godschalk, A., Terouz, S., Briels, C., Larouche, S., Bourbonnière, L., et al.**, Focal disturbances in the blood-brain barrier are associated with formation of neuroinflammatory lesions. *Neurobiol. Dis.* 2015. **74**: 14–24.

4 **Cramer, S. P., Modvig, S., Simonsen, H. J. and Frederiksen, J. L.**, Larsson HB. Permeability of the blood-brain barrier predicts conversion from optic neuritis to multiple sclerosis. *Brain* 2015. **138**: 2571–2583.

5 **Cruciani, C., Puthenparampil, M., Tomas-Ojer, P., Jelcic, I., Docampo, M. J., Planas, R., Manogaran, P., et al.**, T-cell specificity influences disease heterogeneity in multiple sclerosis. *Neurol. Neuroimmunol. Neuroinflamm.* 2021. **8**: e1075.

6 **Heming, M. and Wiendl, H.**, Learning multiple sclerosis immunopathogenesis from anti-CD20 therapy. *Proc. Natl. Acad. Sci. USA* 2023. **120**: e2221544120.

7 **Mansilla, M. J., Presas-Rodriguez, S., Teniente-Serra, A., Gonzalez-Larreategui, I., Quirant-Sanchez, B., Fondelli, F., Djedovic, N., et al.**, Paving the way towards an effective treatment for multiple sclerosis: advances in cell therapy. *Cell. Mol. Immunol.* 2021. **18**: 1353–1374.

8 **Raphael, I., Nalawade, S., Eagar, T. N. and Forsthuber, T. G.**, T cell subsets and their signature cytokines in autoimmune and inflammatory diseases. *Cytokine* 2015. **74**: 5–17.

9 International Multiple Sclerosis Genetics Consortium. electronic address ccye, International Multiple Sclerosis Genetics Consortium. Low-frequency and rare-coding variation contributes to multiple sclerosis risk. *Cell* 2018. **175**: 1679–1687 e7.

10 **Machado-Santos, J., Saji, E., Troscher, A. R., Paunovic, M., Liblau, R., Gabriely, G., Bien, C. G., et al.**, The compartmentalized inflammatory response in the multiple sclerosis brain is composed of tissue-resident CD8+ T lymphocytes and B cells. *Brain* 2018. **141**: 2066–2082.

11 **Tuzlak, S., Dejean, A. S., Iannacone, M., Quintana, F. J., Waisman, A., Ginhoux, F., Korn, T., et al.**, Repositioning T(H) cell polarization from single cytokines to complex help. *Nat. Immunol.* 2021. **22**: 1210–1217.

12 **Thewissen, M., Somers, V., Hellings, N., Fraussen, J., Damoiseaux, J. and Stinissen, P.**, CD4+CD28null T cells in autoimmune disease: pathogenic features and decreased susceptibility to immunoregulation. *J. Immunol.* 2007. **179**: 6514–6523.

13 **van Langelaar, J., van der Vuurst de Vries, R. M., Janssen, M., Wierenga-Wolf, A. F., Spilt, I. M., Siepman, T. A., Dankers, W., et al.**, T helper 17.1 cells associate with multiple sclerosis disease activity: perspectives for early intervention. *Brain* 2018. **141**: 1334–1349.

14 **Schmidt, D., Martens, P. B., Weyand, C. M. and Goronzy, J J.**, The repertoire of CD4+ CD28- T cells in rheumatoid arthritis. *Mol. Med.* 1996. **2**: 608–618.

15 **Liuzzo, G., Goronzy, J. J., Yang, H., Kopecky, S. L., Holmes, D. R., Frye, R. L., Weyand, C. M., et al.**, Monoclonal T-cell proliferation and plaque instability in acute coronary syndromes. *Circulation*. 2000. **101**: 2883–2888.

16 **Namekawa, T., Snyder, M. R., Yen, J. H., Goehring, B. E., Leibson, P. J., Weyand, C. M., Geronzy, J. J., et al.**, Killer cell activating receptors function as costimulatory molecules on CD4+CD28null T cells clonally expanded in rheumatoid arthritis. *J. Immunol.* 2000. **165**: 1138–1145.

17 **Appay, V., Zaunders, J. J., Papagno, L., Sutton, J., Jaramillo, A., Waters, A., Easterbrook, P., et al.**, Characterization of CD4(+) CTLs ex vivo. *J. Immunol.* 2002. **168**: 5954–5958.

18 **Hoeks, C. D., Duran, G., Hellings, N. and Broux, B.**, When helpers go above and beyond: development and characterization of cytotoxic CD4+ T cells. *Front. Immunol.* 2022. **13**.

19 **Hoeks, C. V., Vanheusden, M., Peeters, L. M. Stinissen, P., Broux, B. and Hellings, N.**, Treg-resistant cytotoxic CD4(+) T cells dictate T helper cells in their vicinity: TH17 skewing and modulation of proliferation. *Int. J. Mol. Sci.* 2021. **22**.

20 **Namekawa, T., Wagner, U. G., Goronzy, J. J. and Weyand, C M.**, Functional subsets of CD4 T cells in rheumatoid synovitis. *Arthritis Rheum.* 1998. **41**: 2108–2116.

21 **Ruck, T., Bittner, S., Gross, C. C., Breuer, J., Albrecht, S., Korr, S., Göbel, K., et al.**, CD4+NKG2D+ T cells exhibit enhanced migratory and encephalitogenic properties in neuroinflammation. *PLoS One* 2013. **8**: e81455.

22 **Stopnicki, B., Blain, M., Cui, Q. L., Kennedy, T. E., Antel, J. P., Healy, L. M., Darlington, P. J., et al.**, Helper CD4 T cells expressing granzyme B cause glial fibrillary acidic protein fragmentation in astrocytes in an MHCII-independent manner. *Glia* 2019. **67**: 582–593.

23 **Peeters, L. M., Vanheusden, M., Somers, V., Van Wijmeersch, B., Stinissen, P., Broux, B., Hellings, N., et al.**, Cytotoxic CD4+ T cells drive multiple sclerosis progression. *Front. Immunol.* 2017. **8**: 1160.

24 **Broux, B., Pannemans, K., Zhang, X., Markovic-Plese, S., Broekmans, T., Eijnde, B. O., Wijmeersch, B. V., et al.**, CX(3)CR1 drives cytotoxic CD4(+)CD28(-) T cells into the brain of multiple sclerosis patients. *J. Autoimmun.* 2012. **38**: 10–19.

25 **Zaguia, F., Saikali, P., Ludwin, S., Newcombe, J., Beauseigle, D., McCrea, E., Duquette, P., et al.**, Cytotoxic NKG2C+ CD4 T cells target oligodendrocytes in multiple sclerosis. *J. Immunol.* 2013. **190**: 2510–2518.

26 **Hsiao, C. C., Engelenburg, H. J., Jongejan, A., Zhu, J., Zhang, B., Mingueneau, M., Moerland, P. D., et al.**, Osteopontin associates with brain T(RM)-cell transcriptome and compartmentalization in donors with and without multiple sclerosis. *iScience* 2023. **26**: 105785.

27 **Ramesh, R., Kozhaya, L., McKevitt, K., Djuretic, I. M., Carlson, T. J., Quintero, M. A., McCauley, J. L., et al.**, Pro-inflammatory human Th17 cells selectively express P-glycoprotein and are refractory to glucocorticoids. *J. Exp. Med.* 2014. **211**: 89–104.

28 **Koetzier, S. C., van Langelaar, J., Blok, K. M., van den Bosch, T. P. P., Wierenga-Wolf, A. F., Melief, M. J., Pol, K., et al.**, Brain-homing CD4(+) T cells display glucocorticoid-resistant features in MS. *Neurol. Neuroimmunol. Neuroinflamm.* 2020. **7**.

29 **Jamann, H., Cui, Q. L., Desu, H. L., Pernin, F., Tastet, O., Halaweh, A., Farzam-Kia, N., et al.**, Contact-dependent granzyme B-mediated cytotoxicity of Th17-polarized cells toward human oligodendrocytes. *Front. Immunol.* 2022. **13**: 850616.

30 **Langrish, C. L., Chen, Y., Blumenschein, W. M., Mattson, J., Basham, B., Sedgwick, J. D., McClanahan, T., et al.**, IL-23 drives a pathogenic T cell population that induces autoimmune inflammation. *J. Exp. Med.* 2005. **201**: 233–240.

31 **Koetzier, S. C., Neuteboom, R. F., Wierenga-Wolf, A. F., Melief, M. J., de Mol, C. L., van Rijswijk, A., Dik, W. A., et al.**, Effector T helper cells are

selectively controlled during pregnancy and related to a postpartum relapse in multiple sclerosis. *Front. Immunol.* 2021. **12**: 642038.

32 **Mucida, D., Husain, M. M., Muroi, S., van Wijk, F., Shinnakasu, R., Naoe, Y., Reis, B. S., et al.**, Transcriptional reprogramming of mature CD4$^+$ helper T cells generates distinct MHC class II-restricted cytotoxic T lymphocytes. *Nat. Immunol.* 2013. **14**.

33 **Reis, B. S., Rogoz, A., Costa-Pinto, F. A., Taniuchi, I. and Mucida, D.**, Mutual expression of the transcription factors Runx3 and ThPOK regulates intestinal CD4(+) T cell immunity. *Nat. Immunol.* 2013. **14**: 271–280.

34 **Serroukh, Y., Gu-Trantien, C., Hooshiar Kashani, B., Defrance, M., Vu Manh, T. P., Azouz, A., Detavernier, A., et al.**, The transcription factors Runx3 and ThPOK cross-regulate acquisition of cytotoxic function by human Th1 lymphocytes. *eLife*. 2018. **7**.

35 **Thompson, A. J., Banwell, B. L., Barkhof, F., Carroll, W. M., Coetzee, T., Comi, G., Correale, J., Fazekas, F.**, et al., Diagnosis of multiple sclerosis: 2017 revisions of the McDonald criteria. *Lancet Neurol.* 2018. **17**: 162–173.

36 **Sallusto, F., Zielinski, C. E. and Lanzavecchia, A.**, Human Th17 subsets. *Eur. J. Immunol.* 2012. **42**: 2215–2220.

37 **Paulissen, S. M., van Hamburg, J. P., Dankers, W. and Lubberts, E.**, The role and modulation of CCR6+ Th17 cell populations in rheumatoid arthritis. *Cytokine*. 2015. **74**: 43–53.

38 **Hermans, D., Houben, E., Baeten, P., Slaets, H., Janssens, K., Hoeks, C., Hosseinkhani, B., et al.**, Oncostatin M triggers brain inflammation by compromising blood-brain barrier integrity. *Acta Neuropathol.* 2022. **144**: 259–281.

39 **Van Gassen, S., Callebaut, B., Van Helden, M. J., Lambrecht, B. N., Demeester, P., Dhaene, T. and Saeys, Y.** FlowSOM: Using self-organizing maps for visualization and interpretation of cytometry data. *Cytometry, Part A* 2015. **87**, 636–645. Portico.

40 **Herich, S., Schneider-Hohendorf, T., Rohlmann, A., Khaleghi Ghadiri, M., Schulte-Mecklenbeck, A., Zondler, L., Janoschka, C., et al.**, Human CCR5high effector memory cells perform CNS parenchymal immune surveillance via GZMK-mediated transendothelial diapedesis. *Brain* 2019. **142**: 3411–3427.

41 **Vanheusden, M., Broux, B., Welten, S. P. M., Peeters, L. M., Panagioti, E., Van Wijmeersch, B., Somers, V., et al.**, Cytomegalovirus infection exacerbates autoimmune mediated neuroinflammation. *Sci. Rep.* 2017. **7**: 663.

42 **Nishihara, H., Soldati, S., Mossu, A., Rosito, M., Rudolph, H., Muller, W. A., Latorre, D., et al.**, Human CD4(+) T cell subsets differ in their abilities to cross endothelial and epithelial brain barriers in vitro. *Fluids Barriers CNS*. 2020. **17**: 3.

43 **Lassmann, H.**, Pathogenic mechanisms associated with different clinical courses of multiple sclerosis. *Front. Immunol.* 2018. **9**: 3116.

44 **Kunkl, M., Frascolla, S., Amormino, C., Volpe, E.** and **T L.**, T helper cells: the modulators of inflammation in multiple sclerosis. *Cells*. 2020. **9**.

45 **Raveney, B. J. E., Sato, W., Takewaki, D., Zhang, C., Kanazawa, T., Lin, Y., Okamoto, T., et al.**, Involvement of cytotoxic Eomes-expressing CD4(+) T cells in secondary progressive multiple sclerosis. *Proc. Natl. Acad. Sci. USA.* 2021. **118**.

46 **Glatigny, S., Duhen, R., Oukka, M. and Bettelli, E.**, Cutting edge: loss of alpha4 integrin expression differentially affects the homing of Th1 and Th17 cells. *J. Immunol.* 2011. **187**: 6176–6179.

47 **Steinman, L.**, The discovery of natalizumab, a potent therapeutic for multiple sclerosis. *J. Cell. Biol.* 2012. **199**: 413–416.

48 **Koetzier, S. C., van Langelaar, J., Melief, M. J., Wierenga-Wolf, A. F., Corsten, C. E. A., Blok, K. M., Hoeks, C., et al.**, Distinct effector programs of brain-homing CD8(+) T cells in multiple sclerosis. *Cells*. 2022. **11**.

49 **van Langelaar, J., Rijvers, L., Janssen, M., Wierenga-Wolf, A. F., Melief, M. J., Siepman, T. A., de Vries, H. E., et al.**, Induction of brain-infiltrating T-bet-expressing B cells in multiple sclerosis. *Ann. Neurol.* 2019. **86**: 264–278.

50 **Iannetta, M., Zingaropoli, M. A., Bellizzi, A., Morreale, M., Pontecorvo, S., D'Abramo, A., Oliva, A., et al.**, Natalizumab affects T-cell phenotype in multiple sclerosis: implications for JCV reactivation. *PLoS One*. 2016. **11**: e0160277.

51 **Janoschka, C., Lindner, M., Koppers, N., Starost, L., Liebmann, M., Eschborn, M., Schneider-Hohendorf, T., et al.**, Enhanced pathogenicity of Th17 cells due to natalizumab treatment: implications for MS disease rebound. *Proc. Natl. Acad. Sci. USA.* 2023. **120**: e2209944120.

52 **Raveney, B. J., Oki, S., Hohjoh, H., Nakamura, M., Sato, W., Murata, M., Yamamura, T., et al.**, Eomesodermin-expressing T-helper cells are essential for chronic neuroinflammation. *Nat. Commun.* 2015. **6**: 8437.

53 **Cruz-Guilloty, F., Pipkin, M. E., Djuretic, I. M., Levanon, D., Lotem, J., Lichtenheld, M. G., Groner, Y., et al.**, Runx3 and T-box proteins cooperate to establish the transcriptional program of effector CTLs. *J. Exp. Med.* 2009. **206**: 51–59.

54 **Choi, I. K., Wang, Z., Ke, Q., Hong, M., Qian, Y., Zhao, X., Liu, Y., et al.**, Signaling by the Epstein-Barr virus LMP1 protein induces potent cytotoxic CD4(+) and CD8(+) T cell responses. *Proc. Natl. Acad. Sci. USA.* 2018. **115**: E686–E695.

55 **Schafflick, D., Xu, C. A., Hartlehnert, M., Cole, M., Schulte-Mecklenbeck, A., Lautwein, T., Wolbert, J., et al.**, Integrated single cell analysis of blood and cerebrospinal fluid leukocytes in multiple sclerosis. *Nat. Commun.* 2020. **11**: 247.

56 **Gruarin, P., Maglie, S., De Simone, M., Haringer, B., Vasco, C., Ranzani, V., Bosotti, R., et al.**, Eomesodermin controls a unique differentiation program in human IL-10 and IFN-gamma coproducing regulatory T cells. *Eur. J. Immunol.* 2019. **49**: 96–111.

57 **Bitsch, A., Schuchardt, J., Bunkowski, S. and Kuhlmann, T. and Bruck, W.**, Acute axonal injury in multiple sclerosis. Correlation with demyelination and inflammation. *Brain* 2000. **123**: 1174–1183.

58 **Broux, B., Stinissen, P. and Hellings, N.**, Which immune cells matter? The immunopathogenesis of multiple sclerosis. *Crit. Rev. Immunol.* 2013. **33**: 283–306.

59 **Nakajima, T., Schulte, S., Warrington, K. J., Kopecky, S. L., Frye, R. L., Goronzy, J. J. and Weyand, C. M.**, T-cell-mediated lysis of endothelial cells in acute coronary syndromes. *Circulation* 2002. **105**: 570–575.

60 **Korn, T., Reddy, J., Gao, W., Bettelli, E., Awasthi, A., Petersen, T. R. and Bäckström, B. T.**, Myelin-specific regulatory T cells accumulate in the CNS but fail to control autoimmune inflammation. *Nat. Med.* 2007. **13**: 423–431.

61 **Bailey-Bucktrout, S. L., Martinez-Llordella, M., Zhou, X., Anthony, B., Rosenthal, W., Luche, H. and Fehling, H. J.**, Self-antigen-driven activation induces instability of regulatory T cells during an inflammatory autoimmune response. *Immunity* 2013. **39**: 949–962.

62 **Ifergan, I., Kebir, H., Bernard, M., Wosik, K., Dodelet-Devillers, A., Cayrol, R. and Arbour, N.**, The blood-brain barrier induces differentiation of migrating monocytes into Th17-polarizing dendritic cells. *Brain* 2008. **131**: 785–799.

63 **Bouwman, A. C., van Daalen, K. R., Crnko, S., Ten Broeke, T. and Bovenschen, N.**, Intracellular and extracellular roles of granzyme K. *Front. Immunol.* 2021. **12**: 677707.

64 **Rahman, M. T., Ghosh, C., Hossain, M., Linfield, D., Rezaee, F., Janigro, D., Marchi, N., et al.**, IFN-gamma, IL-17A, or zonulin rapidly increase the permeability of the blood-brain and small intestinal epithelial barriers: relevance for neuro-inflammatory diseases. *Biochem. Biophys. Res. Commun.* 2018. **507**: 274–279.

65 **Markovic-Plese, S., Cortese, I., Wandinger, K. P., McFarland, H. F. and Martin, R.**, CD4+CD28- costimulation-independent T cells in multiple sclerosis. *J. Clin. Invest.* 2001. **108**: 1185–1194.

66 **Broux, B., Mizee, M. R., Vanheusden, M., van der Pol, S., van Horssen, J., Van Wijmeersch, B., Somers, V., et al.**, IL-15 amplifies the pathogenic properties of CD4+CD28- T cells in multiple sclerosis. *J. Immunol.* 2015. **194**: 2099–2109.

67 **Takeuchi, A., Badr Mel, S., Miyauchi, K., Ishihara, C., Onishi, R., Guo, Z., Sasaki, Y., et al.**, CRTAM determines the CD4+ cytotoxic T lymphocyte lineage. *J. Exp. Med.* 2016. **213**: 123–138.

68 **Reboldi, A., Coisne, C., Baumjohann, D., Benvenuto, F., Bottinelli, D., Lira, S., Uccelli, A., et al.**, C-C chemokine receptor 6-regulated entry of TH-17 cells into the CNS through the choroid plexus is required for the initiation of EAE. *Nat. Immunol.* 2009. **10**: 514–523.

69 **Patil, V. S., Madrigal, A., Schmiedel, B. J., Clarke, J., O'Rourke, P., de Silva, A. D., Harris, E., et al.**, Precursors of human CD4(+) cytotoxic T lymphocytes identified by single-cell transcriptome analysis. *Sci. Immunol.* 2018. **3**: eaan8664.

Abbreviations: **BBB**: blood–brain barrier · **CNS**: central nervous system · **CSF**: cerebrospinal fluid · **CTLs**: cytotoxic T cells · **EC**: endothelial cell · **Eomes**: Eomesodermin · **GZMB**: granzyme B · **GZMK**: granzyme K · **NK**: natural killer · **NTZ**: natalizumab · **Runx3**: runt-related transcription factor 3 · **UBiLim**: University Biobank Limburg

Full correspondence: Dr. Marvin M. van Luijn, Department of Immunology, MS Center ErasMS, Erasmus MC, University Medical Center Rotterdam, Wytemaweg 80, 3015 CN, room Nb-1142a, Rotterdam, the Netherlands.
e-mail: m.vanluijn@erasmusmc.nl

Received: 28/4/2023
Revised: 22/11/2023
Accepted: 24/11/2023
Accepted article online: 27/11/2023